




RESEARCH ARTICLE

Influences of passive intervertebral range of motion on cervical vertebral form

Neysa Grider-Potter¹  | Thierra K. Nalley²  | Nathan E. Thompson³  |
Ryosuke Goto¹ | Yoshihiko Nakano¹

¹Graduate School of Human Sciences, Osaka University, Suita, Osaka, Japan

²Department of Medical Anatomical Sciences, Western University of Health Sciences, College of Osteopathic Medicine of the Pacific, Pomona, California

³Department of Anatomy, New York Institute of Technology, College of Osteopathic Medicine, Old Westbury, New York

Correspondence

Neysa Grider-Potter, Graduate School of Human Sciences, Osaka University, Suita, Osaka 565-0871, Japan.
Email: neysagp@gmail.com

Funding information

American Association of Anatomists; Arizona State University; Japan Society for the Promotion of Science, Grant/Award Number: SP15021; National Science Foundation, Grant/Award Numbers: 0935321, 1515271, 1731142

Abstract

Objectives: The cervical spine is the junction between the head and trunk, and it therefore facilitates head mobility and stability. The goal of this study is to test several predictions regarding cervical morphology and intervertebral ranges of motion.

Materials and Methods: Intervertebral ranges of motion for 12 primate species were collected via radiographs or taken from the literature. Morphometric data describing functionally relevant aspects of cervical vertebral morphology were obtained from museum specimens representing these species. We tested for correlations between intervertebral movement and vertebral form using phylogenetic generalized least-squares regression.

Results: Results demonstrate limited support for the hypothesis that range of motion (ROM) is influenced by cervical vertebral morphology. Few morphological variables correlate with ROM and no relationship is consistently significant across cervical joints.

Discussion: These results indicate that the relationship between vertebral morphology and joint ranges of motion is, at most, weak, providing little support the use of bony morphology to reconstruct axial mobility in fossil specimens. Future work should investigate the role of soft tissues in vertebral joint stability.

KEYWORDS

cervical vertebrae, range of motion

1 | INTRODUCTION

The ability to move the head independently of the trunk is an important function of the neck. The decoupling between head and body postures facilitates many aspects of locomotor, social, and dietary behaviors. For example, the neck can stabilize the head when the trunk moves during locomotion, and it can also move the head on a stationary trunk to locate the source of an external stimulus. Correlations between cervical vertebral morphology and positional behavior (i.e., neck posture and/or locomotor mode) across primates have been detected in previous work (Manfreda, Mitteroecker, Bookstein, & Schaefer, 2006; Meyer, Woodward, Tims, & Bastir, 2018; Nalley, 2013; Nalley & Grider-Potter, 2015, 2017). These studies have

focused their interpretations of cervical variation within the context of locomotor differences but have yet to test these inferences directly. For example, Nalley and Grider-Potter (2015) argue that the craniocaudally longer cervical vertebral bodies found in more pronograde primates may serve to increase neck flexion-extension. Yet, the neck supports the head during many other behaviors (e.g., grooming, food processing) unrelated to locomotion which complicates inferred form-function relationships. The aim of this research is to investigate how variation in cervical vertebral form correlates with differences in head and neck ranges of motion during flexion-extension and lateral bending. Testing hypotheses about the functional consequences of morphological variation will allow future research to strengthen the reconstruction of behaviors in extinct taxa.

Primate cervical vertebrae are typically composed of a vertebral body and neural arch. The first cervical vertebra (C1) is an exception: this element has lost its body, which has become the dens of C2. Adjacent vertebral bodies are joined by stiff, fibrocartilaginous joints that contain intervertebral discs. Cervical vertebrae differ from thoracic and lumbar vertebrae in possessing uncinuate processes on the dorsolateral aspects of the superior margins of the bodies which articulate with the vertebral body above to form synovial uncovertebral joints (Figure 1). These uncinuate processes are thought to restrict lateral and rotation movements. Uncovertebral joints have been modeled to guide flexion–extension movements while also further stabilizing the intervertebral joint during lateral bending (Kapandji, 2008; Milne, 1991). Adjacent vertebrae are also connected by synovial joints formed by paired articular facets on the posterolateral aspects of the neural arch. Muscles attaching to the neural arches (e.g., spinalis, semispinalis, splenius, and suboccipitals) produce head extension when contracted bilaterally and lateral flexion when contracted unilaterally. Head–neck flexion is largely produced by the longus capitis, and longus colli muscles, which run along the ventral vertebral bodies and transverse processes, and by the scalene and sternocleidomastoid muscles (Figure 2). Joint stability can be maintained by both ligaments and muscular contraction (Jonas & Wilke, 2018; Kapandji, 2008).

Only a few studies have attempted to relate cervical form to neck function across primates (Ankel, 1972; Gómez-Olivencia et al., 2013; Gommery, 2000; Schultz, 1942, 1961; Toerien, 1961), and even fewer have tested functional hypotheses in a comparative biomechanical framework (Manfreda et al., 2006; Meyer et al., 2018; Nalley, 2013; Nalley & Grider-Potter, 2015, 2017; Parks, 2012). Some of these studies have had some success in understanding the influences of locomotion on vertebral morphology (Manfreda et al., 2006; Meyer et al., 2018; Nalley, 2013), but the use of categorical estimates of locomotor behavior has imposed

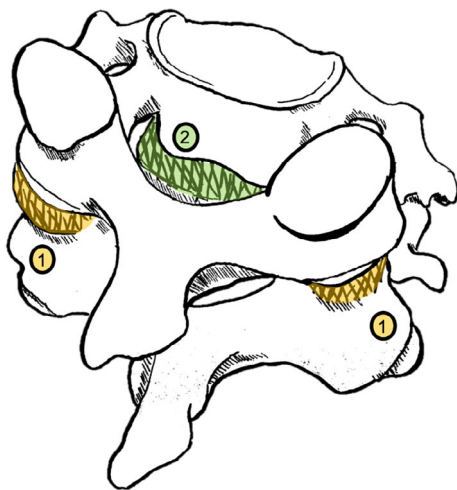


FIGURE 1 Cervical vertebrae articulate at two articular facets along the neural arch via synovial joints (1, yellow) with adjacent vertebral bodies forming the fibrocartilaginous uncovertebral joints (2, green)

limitations to connecting form and function. For example, in their geometric morphometric analysis of C1 morphology, Manfreda et al. (2006) did not find a relationship between locomotor categories and concavity of the superior articular facets. In contrast, using continuous data of neck posture during locomotion reveals that high degrees of atlantooccipital joint curvature reflect pronograde neck postures within primates (Grider-Potter & Hallgren, 2013; Nalley & Grider-Potter, 2017).

Neck posture during locomotion appears to be a suitable measure of neck locomotor function. Strait and Ross (1999) measured the inclination of the mid-neck in the sagittal plane at mid-stance/mid-swing in 29 species of primate. This measure of neck posture can vary between 48 and 107° during quadrupedal locomotion (Strait & Ross, 1999). Variation among the species in this sample suggests that the categories typically used in analyses of primate locomotion do not provide a good proxy for the functional influences on axial morphology. Using Strait and Ross's (1999) data set, Nalley and Grider-Potter (2015, 2017) demonstrated that certain aspects of cervical morphology—spinous process length (SPL), laminar cross-sectional area, vertebral body length, and articular facet angle—correlate with angular inclination of the neck in the sagittal plane during locomotion. Importantly, the neck facilitates head movement during many other behaviors, such as predator vigilance, feeding, foraging, and grooming. A comprehensive understanding of the functional influences on cervical morphology should account for the multifarious functions of the neck, not just sagittal-plane neck posture during locomotion. Facilitating head mobility is one such function, yet little comparative data on head–neck range of motion (ROM) exist that can be used to establish such function inferences.

Absolute head and neck ROM has been quantified in only four species of nonhuman primates (Graf, de Waele, & Vidal, 1995). Graf et al. (1995) conducted one of the few joint-motion studies that include nonhuman mammals. Using radiographs and dissections, they determined that mammalian quadrupeds (*Lepus*, *Felis*, and *Cavia*) have atlantooccipital joint ROM averaging between 92 and 106° of flexion–extension. Interestingly, the primates in their small sample had much smaller ranges: 1.5° in *Macaca fascicularis*, 19° in *Saimiri*, and 32° in *Macaca mulatta* (Graf et al., 1995). *Sapajus apella* was also used in the study but range of flexion was not reported. Although these data are important, the sample is small and unevenly distributed both functionally and phylogenetically, making it difficult to draw general conclusions about the relationship between mammalian cervical form and cervical function.

The goal of this study is to test the hypothesis that bony cervical vertebral morphology influences maximum passive ranges of motion in a sample of primates that practice a variety of locomotor modes and represent major primate clades. From this broader hypothesis, we outline several predictions (Figure 3):

P1: Spinous processes will inhibit extension (Kapandji, 2008). Greater maximum ranges of intervertebral extension at vertebral levels will be associated with shorter spinous processes. Additionally, greater ranges of extension will be associated with more cranially oriented spinous processes, because this orientation prevents spinous

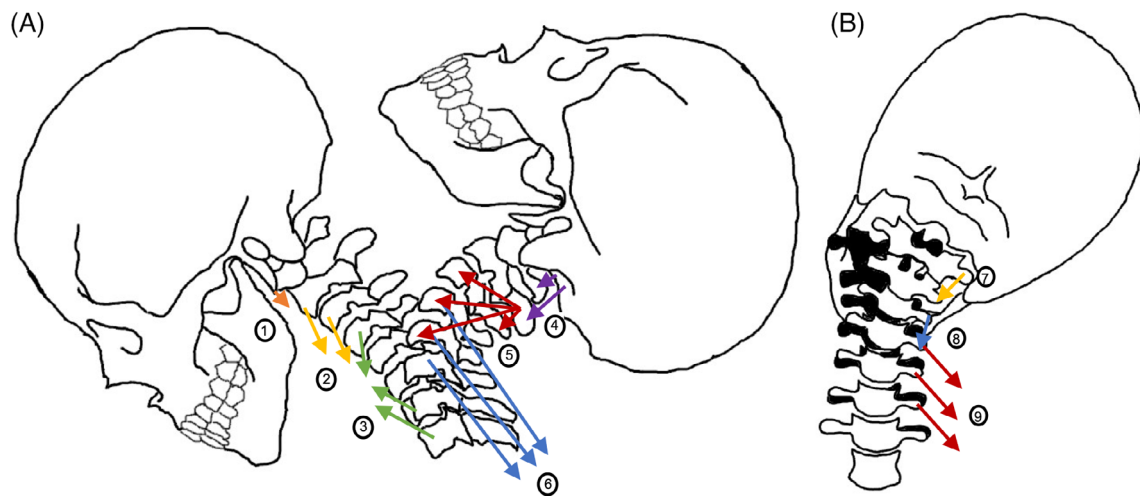


FIGURE 2 Adapted from Kapandji, 2008. (a) Diagram illustrates major muscle groups with cervical attachments that facilitate flexion and extension of the cervical spine. Group 1 (orange arrow) represents the rectus capitis anterior muscles. Group 2 (yellow arrows) represents the longus capitis muscles. Group 3 (green arrows) represents the pair of longus coli muscles. Group 4 (purple arrows) represents the posterior suboccipital group (rectus capitis posterior major and minor muscles). Group 5 represents transversospinales and interspinales muscles. Group 6 represents the erector spinae muscles. (b) Diagram illustrates muscle groups with cervical attachments that facilitate lateral bending of the cervical spine. Group 7 (yellow arrow) represents the suboccipital group (rectus capitis lateralis and obliquus capitis superior muscles). Group 8 (blue arrow) represents the intertransversarii muscles. Group 9 (red arrows) represents the scalene muscle group. Note the possible muscles not found in humans (e.g., atlantoscularis) are not depicted

processes from colliding during maximum extension than a more caudal orientation.

P2: Longer, more caudally oriented transverse processes will inhibit lateral flexion, similar to the relationship predicted for spinous-process orientation and neck extension. Greater ranges of lateral flexion will occur at vertebral levels with shorter, more cranially oriented transverse processes.

P3: Uncinate processes will inhibit lateral flexion (Kapandji, 2008). Vertebral levels with taller uncinate processes will have smaller ranges of lateral flexion.

P4: Larger joint surfaces will increase ROM (Hamrick, 1996). Larger ranges of flexion-extension will occur at intervertebral levels with craniocaudally longer articular facets.

P5: Greater curvature of the atlantooccipital joint will be associated with greater ranges of flexion-extension (Aiello & Dean, 2002; Hamrick, 1996).

2 | METHODS

2.1 | Maximum range of motion

Data on maximum passive ranges of motion between cervical vertebrae, between C1 and the occipital condyles (C0), and between C7 and the first thoracic vertebra (T1) were measured on seven species of primate ($n = 18$ individuals; Tables 1 and 2). The methods used were approved by the institutional animal care and use committee responsible for each animal (Protocol # A141-16-06, Duke University; 27-3-2, Osaka University; 2009-1731-R1 USDA, Stony Brook University). Individuals were anesthetized and then gently but firmly moved

into their maximum ranges of flexion, extension, and lateral flexion. Sandbags were used to hold individuals in position for radiography. Because the anesthesia mask often prohibited the chin from touching the chest, it was momentarily removed to achieve maximum flexion during imaging. A neutral posture was also radiographed to separate flexion and extension. This neutral posture was defined by orienting the neck parallel to the trunk and allowing the head to fall naturally. The chimpanzee data set does not include a neutral posture or lateral flexion and was therefore only included in the flexion-extension analysis. A neutral posture for lateral flexion was not radiographed in any taxa and methods to measure total ROM in the coronal are further described below.

To measure ROM in the sagittal plane, maximum flexion and extension radiographs were overlain with the neutral posture at T2. Lines were drawn along the articular pillars, which are quite dense and thus easily visible. Angles were taken between the same vertebrae in these different positions using ImageJ (Schneider, Rasband, & Eliceiri, 2012) to obtain intervertebral ranges of motion (Figure 4). The total ROM in the sagittal plane (flexion-extension) was obtained by summing ranges of flexion and extension for each individual. The neutral position in the coronal plane was assumed to be at midline. Thus, angles were measured between vertebrae at maximum lateral flexion, with the orientation of T1 vertebral body used as the neutral posture because it is assumed to be parallel (0°) with the rest of the spine in neutral position.

Limited ROM data are also available in the literature. Human ROM is well established in the medical literature (White & Panjabi, 1990). As discussed, Graf et al. (1995) measured intervertebral ranges of motion in four species of primate: *M. mulatta*, *M. fascicularis*, *S. sciureus*, and *S. apella*. Graf et al. collected their data from

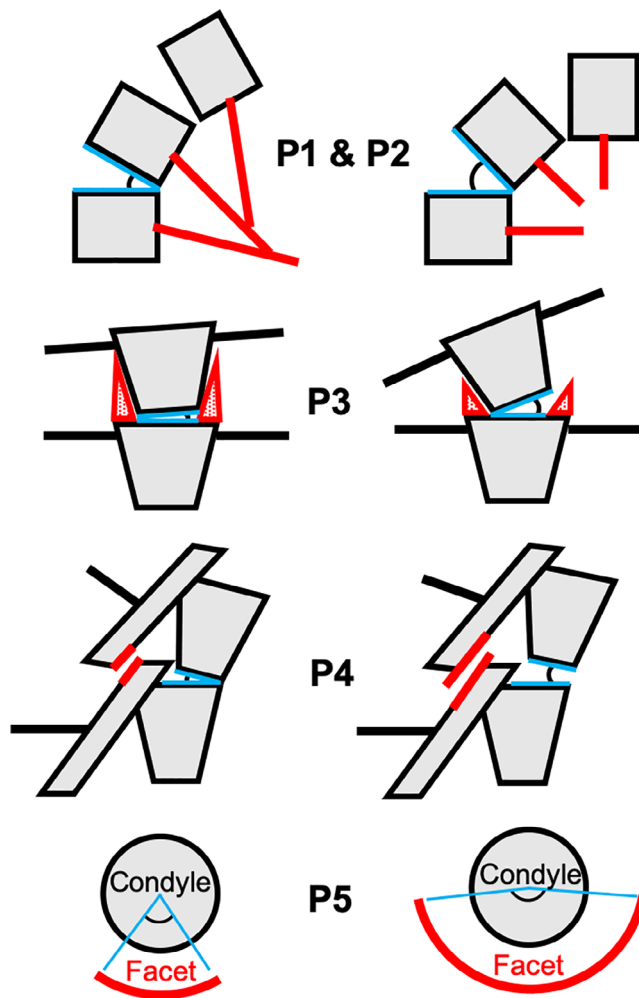


FIGURE 3 Models depicting Predictions 1–5. Morphologies producing smaller range of motion (ROM) on the left and those producing larger ROM on the right

radiographs of anesthetized animals and, with the exception of the C0–C1 joint, their measurements appear to be analogous to the data collected for this study. These data were included in the analyses, with the exception of the C0–C1 measurements, whose 200+ degree values are much larger than those collected for this study which do not exceed 65° (see Tables 1 and 2 for complete list). The taxa included in our study represent a diverse range of species, locomotor repertoires, and postural habits found in extant primates.

2.2 | Morphological data

Morphological data were collected from 676 vertebrae, representing levels C1–T1, from osteological specimens housed at the American Museum of Natural History (New York, NY), National Museum of Natural History (Washington, DC), Muséum National de l'Histoire Naturelle (Paris, France), and Field Museum of Natural History (Chicago, IL) (Table 1). The selection of taxa was dictated by the species for which ROM data were available. Only adult specimens were used, with maturity of individuals being

TABLE 1 List of species included in the ROM and morphological samples. For each species, the number of specimens for each variable is provided separately (n_{ROM} and n_{Morph} , respectively). Sample sizes for data taken from Graf et al. (1995) are listed as approximate because those authors did not report number of specimens per species. Our approximations are based on the total number of primates ($n = 10$) and the fact that only one *S. apella* was used. Therefore, the number of individuals for their other species must be between 2 and 4

Species	n_{ROM}	ROM source	n_{Morph}
<i>Eulemur mongoz</i>	3	Duke Lemur Center	6
<i>Lemur catta</i>	3	Duke Lemur Center	7
<i>Propithecus verreauxi</i>	3	Duke Lemur Center	9
<i>Otolemur crassicaudatus</i>	1	Duke Lemur Center	8
<i>V. variegata</i>	3	Duke Lemur Center	9
<i>M. mulatta</i>	~3	Graf et al. (1995)	15
<i>M. fascicularis</i>	~3	Graf et al. (1995)	7
<i>S. apella</i>	1	Graf et al. (1995)	8
<i>S. sciureus</i>	~3	Graf et al. (1995)	9
<i>Hylobates lar</i>	1	Osaka University	8
<i>P. troglodytes</i>	2	Stony Brook University	13
<i>H. sapiens</i>	NA	White and Panjabi (1990)	6

Abbreviation: ROM, range of motion.

determined based on the fusion of annular rings. Because all ROM data came from captive individuals, geographical origin of the specimens was not assessed.

Morphometric data were collected from landmarks acquired in two ways. First, three-dimensional (3D) surface scans of some specimens were obtained using an Einscan 3Ds (Shining 3D) white-light scanner. This scanner has an accuracy of <0.05 mm. Landmarks (Figure 5) were placed on the scans using Rhinoceros (McNeel and Associates) CAD software, and linear measurements were acquired by computing interlandmark distances (Figure 5, Table 3). Second, for the remaining specimens, the same set of landmarks was digitized using a Microscribe (Immersion Corp.) and measurements were obtained as for the scanned specimens (Figure 5, Table 3). Measurements were taken from the left side unless absent or degraded, in which case the right side was used. The C6 typically has anterior and posterior tubercles. Both tubercles are occasionally present in C5 and C7 levels as well, depending on the species. In C5 and C6, the anterior tubercle is always longer and more robust, whereas the reverse is true for C7. For our purposes, the longer process was used for analysis under the assumption that the more robust structure has a stronger influence on ROM.

Using Rhinoceros, a plane was fit to 8–12 semilandmarks which were digitized along the margins of the cranial surface of the vertebral body for C3–T1. Angular measurements were taken relative to a line perpendicular to this plane. Because C2 lacks this cranial surface, its angular measurements were taken relative to a line between the inferiormost and superiormost aspect of the vertebral body on the

TABLE 2 Species means of cervical joint ranges of extension, flexion, and lateral flexion. The total ROM in the sagittal plane (flexion-extension) was computed but summing flexion and extension. Graf et al.'s (1995) values for C0-C1 (italicized) of *Macaca sp.*, *S. apella*, and *S. sciureus* were not used in the analyses

Species	Joint(s)	Extension	Flexion	Flexion-extension	Lateral flexion
<i>E. mongoz</i>	C0-C1	35.4 ± 7.8	25.9 ± 20.7	61.4 ± 15.6	7.1 ± 6.1
	C1-C2	4.3 ± 3.9	14.4 ± 4.2	18.7 ± 4.0	22.8 ± 10.9
	C2-C3	8.5 ± 6.3	5.1 ± 1.6	13.6 ± 4.6	7.3 ± 1.9
	C3-C4	5.2 ± 4.0	2.9 ± 2.8	8.1 ± 3.5	5.8 ± 3.7
	C4-C5	9.2 ± 2.9	7.8 ± 5.7	17.0 ± 4.5	5.1 ± 3.7
	C5-C6	17.5 ± 6.7	3.2 ± 2.5	20.7 ± 5.1	5.7 ± 1.5
	C6-C7	16.0 ± 10.7	4.7 ± 4.0	20.7 ± 8.1	5.1 ± 1.8
	C7-T1	19.3 ± 11.3	6.6 ± 7.4	26.0 ± 9.6	4.1 ± 1.7
	C0-T1	115.4 ± 7.3	70.8 ± 8.4	186.2 ± 7.9	63.1 ± 5.0
<i>H. sapiens</i>	C0-C1	12.4	14.4	26.8	5.0
	C1-C2	10.5	12.7	23.2	5.0
	C2-C3	2.0	7.0	9.0	10.0
	C3-C4	4.0	10.0	14.0	11.0
	C4-C5	9.0	3.0	12.0	11.0
	C5-C6	3.0	15.0	18.0	8.0
	C6-C7	10.0	9.0	19.0	7.0
	C7-T1	6.0	4.0	10.0	4.0
	C0-T1	56.9	75.1	132.0	61.0
<i>Hylobates lar</i>	C0-C1	11.6	3.2	14.8	6.3
	C1-C2	8.9	4.8	13.7	4.9
	C2-C3	11.9	7.0	18.9	11.7
	C3-C4	11.2	8.7	19.9	2.6
	C4-C5	17.5	0.1	17.6	1.7
	C5-C6	9.1	6.1	15.2	1.7
	C6-C7	11.6	27.2	38.8	1.7
	C7-T1				2.3
	C0-T1				32.9
<i>L. catta</i>	C0-C1	8.9 ± 4	16.8 ± 7	25.8 ± 5.7	8.1 ± 7.8
	C1-C2	8.2 ± 6.1	16.7 ± 6.4	25.0 ± 6.3	28.2 ± 9.8
	C2-C3	8.6 ± 1.9	5.5 ± 0.8	14.1 ± 1.5	6.7 ± 2.8
	C3-C4	7.1 ± 4.3	7.6 ± 5.0	14.7 ± 4.7	7.3 ± 1.6
	C4-C5	10.8 ± 10.7	10.2 ± 2.8	21.0 ± 7.8	5.5 ± 2.9
	C5-C6	17.5 ± 5.2	6.5 ± 3.4	24.0 ± 4.4	6.6 ± 1.7
	C6-C7	23.5 ± 9.8	6.8 ± 2.2	30.3 ± 7.1	4.8 ± 3.2
	C7-T1	14.2 ± 8.8	9.2 ± 5.2	23.3 ± 7.2	3.8 ± 1.9
	C0-T1	98.9 ± 7.0	79.2 ± 4.6	178.1 ± 5.9	71.0 ± 2.9
<i>M. fascicularis</i>	C0-C1	119.3 ± 5.1	118.0 ± 10.1	237.3 ± 8.0	0.0 ± 0.0
	C1-C2	7.0 ± 2.6	5.3 ± 2.1	12.3 ± 2.4	0.0 ± 0.0
	C2-C3	16.0 ± 4.6	8.3 ± 6.7	24.3 ± 5.7	3.0 ± 3.0
	C3-C4	8.0 ± 1.5	5.0 ± 5.6	13.0 ± 4.1	2.7 ± 2.3
	C4-C5	11.3 ± 4.2	0.0 ± 0.0	11.3 ± 3.0	8.0 ± 2.0
	C5-C6	8.6 ± 3.2	0.0 ± 0.0	8.6 ± 2.3	7.0 ± 1.7
	C6-C7	16.7 ± 5.7	0.0 ± 0.0	16.7 ± 4.0	2.7 ± 2.5
	C7-T1	21.3 ± 7.0			
	C0-T1				

(Continues)

TABLE 2 (Continued)

Species	Joint(s)	Extension	Flexion	Flexion-extension	Lateral flexion
<i>M. mulatta</i>	C0-C1	137.0	105.0	242.0	
	C1-C2	3.0	0.0	3.0	
	C2-C3	4.0	20.0	24.0	
	C3-C4	10.0	4.0	14.0	
	C4-C5	13.0	5.0	18.0	
	C5-C6	16.0			
	C6-C7	22.0			
	C7-T1	10.0			
<i>O. crassicaudatus</i>	C0-C1	5.7	13.0	7.3	3.5
	C1-C2	7.1	8.8	1.7	16.3
	C2-C3	7.6	18.1	25.8	7.3
	C3-C4	13.4	3.7	17.1	9.3
	C4-C5	0.8	8.8	9.6	3.4
	C5-C6	15.5	-3.1	12.3	3.4
	C6-C7	1.3	10.6	9.4	5.3
	C7-T1	26.6	2.5	29.0	4.2
	C0-T1	90.5	57.5	119.8	58.4
<i>Pan troglodytes</i>	C0-C1			8.8	
	C1-C2			16.1	
	C2-C3			1.6	
	C3-C4			10.8	
	C4-C5			19.3	
	C5-C6			23.9	
	C6-C7			14.1	
	C7-T1				
	C0-T1				
<i>P. verreauxi</i>	C0-C1	9.5 ± 6.1	19.3 ± 14.7	27.2 ± 11.3	2.6 ± 0.6
	C1-C2	8.5 ± 5.9	11.0 ± 13.2	18.3 ± 10.2	11.5 ± 1.4
	C2-C3	8.6 ± 2.9	6.6 ± 2.1	15.2 ± 2.5	11.4 ± 1.7
	C3-C4	19.6 ± 2.2	6.8 ± 3.6	26.4 ± 3.0	10.1 ± 1.1
	C4-C5	10.6 ± 4.3	7.7 ± 3.7	18.3 ± 4.0	7.4 ± 3.7
	C5-C6	11.6 ± 2.9	9.2 ± 1.4	20.8 ± 2.2	6.5 ± 1.8
	C6-C7	15.6 ± 7.2	6.6 ± 8.1	22.3 ± 7.7	4.3 ± 1.9
	C7-T1	14.5 ± 9.2	3.5 ± 1.8	18.0 ± 6.6	6.2 ± 2.9
	C0-T1	98.5 ± 5.6	70.8 ± 7.8	166.6 ± 6.8	60.0 ± 2.1
<i>S. sciureus</i>	C0-C1	116.4 ± 12.3	106.7 ± 20.2	223.1 ± 16.7	0.0
	C1-C2	22.2 ± 9.4	3.3 ± 5.8	25.5 ± 7.8	7.5
	C2-C3	3.6 ± 2.3	0.7 ± 0.6	4.3 ± 1.7	1.5
	C3-C4	8.6 ± 2.6	0.7 ± 0.6	13.3 ± 4.0	5.0
	C4-C5	11.2 ± 2.3	3.7 ± 4.7	14.9 ± 3.7	0.0
	C5-C6	12 ± 4.0	3.7 ± 0.6	15.7 ± 2.9	0.0
	C6-C7	19 ± 1.6	3.0 ± 1.7	22.0 ± 1.7	6.0
	C7-T1	22.6 ± 8.3	3.0 ± 1.7	25.6 ± 6.0	4.0
	C0-T1				

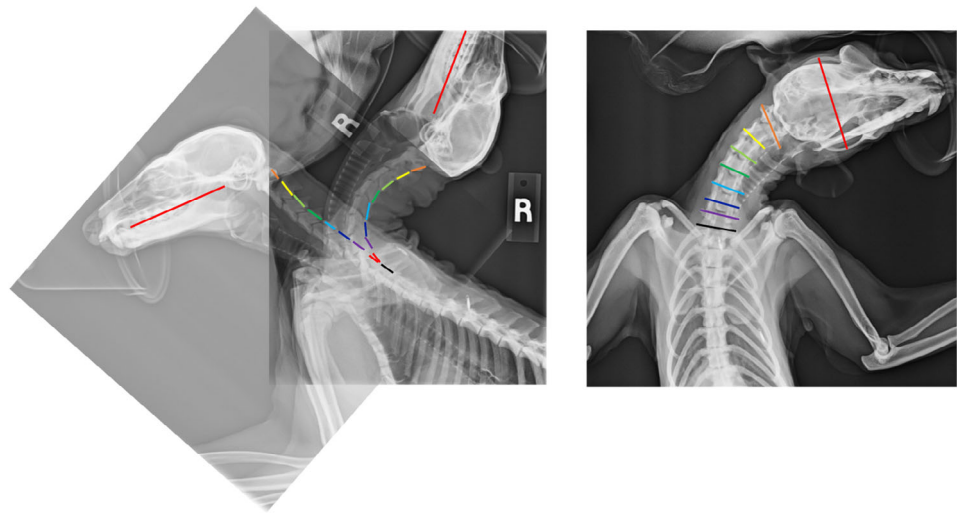
(Continues)

TABLE 2 (Continued)

Species	Joint(s)	Extension	Flexion	Flexion-extension	Lateral flexion
<i>S. apella</i>	C0-C1	107.5			
	C1-C2	0.0			
	C2-C3	0.0			
	C3-C4	1.5			
	C4-C5	0.0			
	C5-C6	2.5			
	C6-C7	20.5			
	C7-T1	6.5			
<i>V. variegata</i>	C0-C1	34.4 ± 12.9	21.7 ± 22.3	56.0 ± 18.1	2.7 ± 1.7
	C1-C2	4.9 ± 4.3	3.0 ± 3.2	7.9 ± 3.8	28.4 ± 10.4
	C2-C3	7.5 ± 5.7	9.2 ± 2.4	16.7 ± 4.4	5.2 ± 2.0
	C3-C4	8.2 ± 4.3	13.3 ± 3.8	21.4 ± 4.1	7.1 ± 4.3
	C4-C5	10 ± 6.7	20.0 ± 3.7	36.0 ± 5.4	9.7 ± 2.4
	C5-C6	11.4 ± 2.8	9.9 ± 2.1	21.3 ± 2.5	5.9 ± 3.6
	C6-C7	18.0 ± 10.9	13.6 ± 3.3	31.5 ± 8.1	5.9 ± 1.9
	C7-T1	13.5 ± 7.5	15.0 ± 8.8	28.4 ± 8.2	4.1 ± 2.1
	C0-T1	113.8 ± 7.6	105.5 ± 8.9	219.3 ± 8.3	69.0 ± 4.5

Abbreviation: ROM, range of motion.

FIGURE 4 *Varecia variegata* radiographs of neutral posture (left) and extension (middle) overlain at T2 (black line). Lateral flexion angles (right) were measured relative to T1 (black line) during lateral flexion. Images were imported into ImageJ to measure the angles between lines



ventral surface at midline (vertebral measurement #9, Figure 5, Table 3). Because the atlas lacks a centrum entirely, only the angle defining atlantooccipital joint curvature was calculated. To measure this angle, two planes were fit to 15–20 semilandmarks along the dorsal and ventral aspects of the joint surface, following Nalley and Grider-Potter (2017) (Figure 5, Table 3).

2.3 | Analytical procedures

Phylogenetic generalized least-squares (PGLS) regression was used to test for correlations between vertebral morphology and intervertebral

ROM. The tree used in the analyses was downloaded from 10krees.nunn-lab.org (Arnold, Matthews, & Nunn, 2010). Analyses were conducted in R using the packages ape (Paradis et al., 2018), geiger (Harmon et al., 2008), and caper (Orme et al., 2013). Most of the morphological variables of interest should affect ROM of the more cranial intervertebral joint. For example, the uncinat processes of C3 should influence the range of lateral flexion in the C2–C3 joint. Thus, all but one of the morphological variables were tested against their cranial joint's ROM. The exception was SPL and angle, which should be more strongly correlated with the caudal joint ROM.

Linear measurements were size adjusted by dividing each by the square root of vertebral canal area. Previous research has

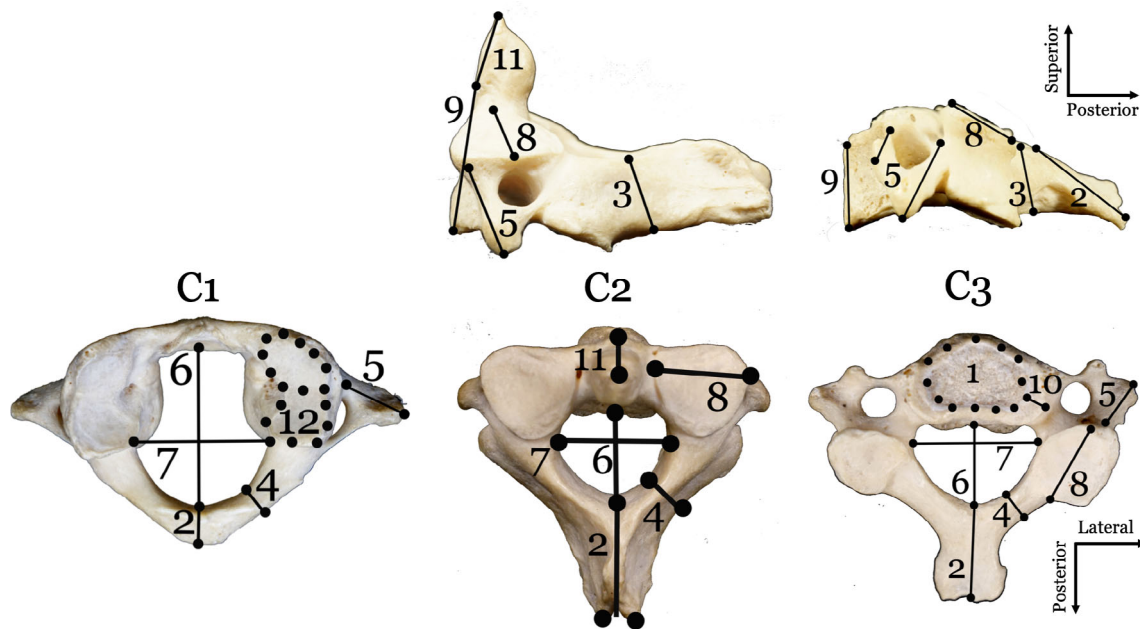


FIGURE 5 Variables measured from skeletal material. Linear measurements calculated based on distances between landmarks. Angular measurements calculated between vertebral body plane (C3-T1), VBH line (C2), and relative to itself (C1, superior articular facet). See Table 2 for descriptions. Human C1 (left), C2 (middle), and C3 (right); lateral (top) and superior (bottom) views

shown canal dimensions to correlate strongly with body mass (Grider-Potter, 2019; MacLarnon, 1996; Nalley, 2013). However, because previous work has observed a relative enlargement of the thoracic canal in the hominoids (Maclarnon & Hewitt, 2004), additional PGLS analyses were conducted in order to ensure that this size surrogate is appropriate. Canal area was calculated using the equation for the area of an ellipse ($A = \pi ab$) where a is the half the width of the canal (Figure 5, Line 7) and b is half its height (Figure 5, Line 6) and species means of body mass was collected from the literature (Smith & Jungers, 1997). As a whole, there is a strong relationship between square root of canal area and body mass (Table 4, Figure 6). The slopes of the relationships are generally within the line of isometry ($m = 1$); however, several are slightly negatively allometric, more so in the female vertebrae than the males. Vertebral body area, a commonly used body size proxy in thoracic and lumbar vertebrae analyses, could not be used due to the lack of a vertebral body on C1 and the presence of uncinate processes on C3-C7, which confounds this measurement. Using canal area as a proxy for organismal size allowed the dimensions to be scaled by vertebral specimen rather than relying on species averages of body mass. These shape ratios were logarithmically transformed prior to analysis. For ROM data taken from the literature, sex was not specified, and a mixed-sex sample was collected from the strepsirrhine portion of the sample. *T* tests were conducted to test for differences in form and function due to sex. No significant differences between male and female morphology (relative to vertebral canal area) or intervertebral ranges of motion and, thus, sexes were analyzed together. To control for multiple testing, *p*-values were adjusted using the false discovery rate (Benjamini & Hochberg, 1995) method, applied within each prediction (Table 3).

3 | RESULTS

Results of the PGLS analyses demonstrate little significance. No results are significant for spinous process angle, transverse process length, uncinate process height, or articular facet angle regressions (Figures 7–9). Only 3 of 43 regressions indicated a significant relationship between cervical morphology and intervertebral ROM. One significant relationship between SPL and intervertebral range of extension was found in the C7–T1 joint (Figure 7). In this joint, range of extension decreases with increasing process length. This relationship was not found at any of the more cranial levels. Only the C4–C5 joint demonstrates a significant association between transverse process angle (TPA) and lateral flexion and no correlations with transverse process length are significant (Figure 8, Table 3). The C4–C5 joint also demonstrated significant correlations between superior articular facet height and range of flexion. Increased facet height was associated with increased range of flexion (Figure 9, Table 3) at that level.

4 | DISCUSSION

Overall, these results do not provide clear support for the hypothesis that bony cervical vertebral morphology influences intervertebral ROM. Only a few levels showed significant correlations between ROM and morphology that are in the predicted direction. Nevertheless, we are hesitant to completely reject the functional hypothesis proposed here. Distinct functional segments of the cervical spine have been identified in the human biomedical literature: the atlantooccipital unit (C0–C1), the craniocervical unit (C1–C2), the

TABLE 3 Vertebral measurements and their descriptions. See Figure 4 for depiction

Measurement	Number	Description
Vertebral body plane	1	Plane fit to 8–12 points along the margin of the cranial aspect of the vertebral body
SPL	2	Maximum length of the spinous process
Lamina height	3	Maximum height of the lamina
Lamina width	4	Maximum width of the lamina
TPL	5	Maximum length of the transverse process
Canal length	6	Maximum length of canal at midline
Canal width	7	Maximum width of vertebral canal
SAFH	8	Maximum height of the superior articular facet
Vertebral body height	9	Maximum height of the ventral aspect of the vertebral body
UH	10	Maximum height of the uncinat process
Dens height	11	Maximum height of the dens
SAFA	12	Angle between the two aspects of C1's superior articular facet. Two planes fit to 15–20 points along the margins of these aspects
SPA	13	Craniocaudal orientation of the spinous process; angle between the SPL line and VBP
TPA	14	Craniocaudal orientation of the transverse process; angle between the TPL line and VBP

Abbreviations: SAFA, superior articular facet angle; SAFH, superior articular facet height; SPA, spinous process angle; SPL, spinous process length; TPA, transverse process angle; TPL, transverse process length; UH, uncinat process height.

root (C2–C3), and the column (C3–C7) (e.g., Jonas & Wilke, 2018; White & Panjabi, 1990). In humans, these functional segments couple during lateral bending and axial rotation: C0–C2 tend to move as a group, as do C2–C5 and C5–T1 (White & Panjabi, 1990). It could be that these functional groups are influencing the results: the C4/C5 joint could demonstrate significance for TPA and articular facet height because the coupling pattern breaks at C5. Further studies should be conducted investigating motion in three-dimensions.

4.1 | Spinous processes

Longer spinous processes appear to inhibit range of extension only in the lowest cervical level (C7–T1). Anecdotally, the lower spinous processes only appear to touch in the radiographs taken from *Pan troglodytes*. Apes have relatively large, straight spinous processes but humans possess short, caudally oriented processes, especially in the

lower cervical levels (Nalley, 2013). It is likely that spinous processes are too short in most of the species examined here to inhibit range of extension.

Nalley and Grider-Potter (2015) found that neck posture strongly correlates with SPL in C3–C7 vertebrae. They used the inclination of the mid-neck during mid-stance or mid-swing, taken from Strait and Ross (1999). Based on their results, Nalley and Grider-Potter (2015) argued that longer spinous processes are required in primates with more horizontal neck postures in order to increase the mechanical advantage of the nuchal musculature. These correlations were high and significant across all levels, indicating that habitual neck postures may more strongly influence cervical morphology than facilitating head mobility, with reduced ROM being a tradeoff of efficiently maintaining head stability in these species.

4.2 | Transverse processes

No significant correlations were found between transverse processes length and lateral flexion. The relationship between TPA and lateral flexion was only significant at one level, C4–C5. Contrary to predictions, the process is more caudally oriented in species with greater range of lateral flexion. This orientation may offer greater mechanical advantage to the lateral flexors. However, any relationship between ROM and moment arm lengths has not been established.

4.3 | Uncinat processes

Uncinat process height also appears to be unrelated to range of lateral flexion. Although they are thought to provide joint stability, it could be that soft tissue more strongly inhibits motion. Meyer et al. (2018) published a geometric morphometric analysis of uncinat process morphology in primates. The results indicated that larger primates tend to have relatively shorter processes than do smaller bodied species. Because there is no known interspecific relationship between body mass and vertebral ROM, this scaling pattern may also indicate a function unrelated to neck mobility.

Given our results, it remains unclear what functional role the uncinat processes play. Previous research has demonstrated that other vertebral features provide joint stability (e.g., the lumbar fibrocartilaginous annulus fibrosis) (Chow, Luk, Evans, & Leong, 1996; Eck et al., 2002; Hilibrand & Robbins, 2004; Kumar, Baklanov, & Chopin, 2001; Rohlmann, Zander, Schmidt, Wilke, & Bergmann, 2006). It is possible that the uncinat process limits the range of rotation, rather than lateral flexion. It is commonly suggested in the literature that the uncinat processes require humans to extend and laterally flex their cervical vertebrae in order to accomplish neck rotation (Kapandji, 2008; White & Panjabi, 1990). Further work using methods such as X-ray reconstruction of moving morphology (XROMM) could clarify the pattern of motion and the role of the uncinat processes, especially during axial rotation.

TABLE 4 Results of the PGLS models testing the relationship between log (Canal Area^(1/2)) and log (Body Mass^(1/3)) per vertebral level and sex. Canal area was calculated from the digitized data described in the methods and species means of body mass was collected from the literature (Smith & Jungers, 1997)

Level/sex	λ	b	m	r^2	p
C1 M	0	2.015 ± 0.082	1.038 ± 0.133	.882	<.001
C2 M	0	1.633 ± 0.063	0.981 ± 0.102	.920	<.001
C3 M	0	1.578 ± 0.048	0.933 ± 0.068	.940	<.001
C4 M	0	1.572 ± 0.053	0.932 ± 0.076	.931	<.001
C5 M	0	1.621 ± 0.058	0.882 ± 0.082	.905	<.001
C6 M	0.239	1.585 ± 0.061	0.922 ± 0.082	.920	<.001
C7 M	0.383	1.634 ± 0.066	0.807 ± 0.088	.875	<.001
C1 F	0	1.988 ± 0.032	1.051 ± 0.056	.972	<.001
C2 F	0.8	1.580 ± 0.073	0.968 ± 0.093	.914	<.001
C3 F	0.233	1.573 ± 0.056	0.875 ± 0.083	.887	<.001
C4 F	0.815	1.576 ± 0.056	0.829 ± 0.063	.925	<.001
C5 F	0.595	1.607 ± 0.048	0.854 ± 0.061	.933	<.001
C6 F	0	1.580 ± 0.055	0.927 ± 0.085	.901	<.001
C7 F	0.76	1.613 ± 0.060	0.786 ± 0.069	.907	<.001

Abbreviations: PGLS, phylogenetic generalized least-squares.

4.4 | Articular facets

Our results found that articular facet height is poorly correlated with intervertebral range of flexion-extension. An alternative explanation suggests that larger facets offer a larger area to distribute shear forces associated with more pronograde postures in primates (Badoux, 1968) rather than influencing ROM. Nalley and Grider-Potter (2015, 2017) also observed a significant correlation between articular facet orientation and neck posture. They found that more coronally oriented facets were typical of more pronograde species, but only at the C4 and C7 vertebral levels. They concluded that these orientations might offer greater resistance to displacement in these taxa. It is likely that both facet orientation and size influence the dissipation of forces at the zygapophyseal joints. The results of this study do indicate the ROM at C4/C5 joint significantly correlates with TPA as well as articular facet height. The fourth cervical vertebra is often at the apex of the cervical lordotic curve and could potentially be under greater constraint as a result.

Our results also indicate that atlantooccipital joint curvature is unrelated to range of flexion-extension. Previous analyses conducted by Nalley and Grider-Potter (2017) have shown significant correlations between joint curvature and neck posture, and, this relationship seems largely driven by changes in the anterior aspect of the facet. The anterior aspect becomes more dorsally oriented in more pronograde species (Grider-Potter & Hallgren, 2013). It is possible that this configuration protects the joint from multidirectional forces experienced in pronograde postures, producing greater facet curvature but not an increase in ROM. Hamrick's (1996) study on primate carpals suggests that joint curvature reflects habitual loading patterns. A relatively flat "female" facet is adapted to dissipating unidirectional

loads whereas a more curved joint may habitually dissipate loads from many directions. It is possible that the curvature of the occipital condyles, the "male" aspect of the C0-C1 joint, is more strongly associated with joint ROM, and that the curvature of the "female" articular facet reflects loading patterns. For example, ROM at the knee may be more strongly reflected by the morphology of the femoral condyles, whereas loading may have a stronger influence on the morphology of the tibial condyles (Hamrick, 1996).

4.5 | The role of ligaments

Ligament function has been investigated within the human medical literature. In particular, step-wise reduction of the ligaments has been a common method to understand their relevant contributions to joint stability. For example, work in the upper part of the human cervical spine by Panjabi, Dvorak, Crisco, et al. (1991) and Panjabi, Dvorak, and Iii (1991) has demonstrated that removing the alar ligament leads to greater ranges of flexion and rotation at the C1-C2 joint. In a study on mid-cervical joint motion, Onan, Heggenes, and Hipp (1998) showed that removing the anterior and posterior longitudinal ligaments and intervertebral disc in humans contributed to greater ranges of flexion-extension while the joint capsule functioned mainly in providing stability during rotational and lateral bending motions. Heuer, Schmidt, Klezl, Claes, and Wilke (2007) conducted a step-wise reduction of the ligaments in the human lumbar spine. They found a significant increase (5–10°) in ranges of motion in all planes when all ligaments were removed.

In this study, we considered ROM data collected in two dimensions, as is typical in the literature on neck motion. Anecdotally, the

TABLE 5 ROM vs. skeletal morphology PGLS results, significant results are in bold

Joint	Motion	Morph	λ	b	m	Adj. r^2	Adj. p
C1-C2	Ext	SPL	0	-1.995 ± 0.377	0.008 ± 0.037	-.136	.838
C2-C3	Ext	SPL	0	-0.223 ± 0.099	0.006 ± 0.013	-.111	.778
C3-C4	Ext	SPL	0	-0.371 ± 0.163	-0.008 ± 0.016	-.086	.778
C4-C5	Ext	SPL	0	-0.573 ± 0.211	0.010 ± 0.018	-.076	.778
C5-C6	Ext	SPL	0	-0.007 ± 0.167	-0.351 ± 0.013	.368	.099
C6-C7	Ext	SPL	0.122	-0.348 ± 0.288	0.012 ± 0.017	-.052	.778
C7-T1	Ext	SPL	0	0.743 ± 0.171	-0.039 ± 0.010	.606	.034
C2-C3	Ext	SPA	0	73.510 ± 23.281	2.694 ± 3.147	-.035	.627
C3-C4	Ext	SPA	0	147.508 ± 11.359	-0.552 ± 1.090	-.090	.627
C4-C5	Ext	SPA	1	160.144 ± 12.596	-0.968 ± 0.853	.031	.579
C5-C6	Ext	SPA	0	129.718 ± 12.234	0.614 ± 0.943	-.068	.627
C6-C7	Ext	SPA	1	143.604 ± 12.758	-1.304 ± 0.664	.241	.342
C7-T1	Ext	SPA	1	121.364 ± 11.675	0.801 ± 0.444	.220	.342
C0-C1	Lat Flex	TPL	0.435	-1.168 ± 1.484	0.010 ± 0.260	-.200	.970
C1-C2	Lat Flex	TPL	0	-2.091 ± 0.922	0.078 ± 0.073	.213	.266
C2-C3	Lat Flex	TPL	0	1.697 ± 1.849	-0.247 ± 0.209	.061	.389
C3-C4	Lat Flex	TPL	1	1.703 ± 0.998	-0.303 ± 0.095	.606	.064
C4-C5	Lat Flex	TPL	0.974	0.829 ± 1.048	-0.226 ± 0.098	.421	.137
C5-C6	Lat Flex	TPL	1	1.761 ± 0.877	-0.460 ± 0.124	.682	.055
C6-C7	Lat Flex	TPL	1	1.460 ± 0.791	-0.493 ± 0.125	.709	.055
C7-T1	Lat Flex	TPL	1	-1.204 ± 2.036	0.093 ± 0.439	-.236	.963
C1-C2	Lat Flex	TPA	0	58.532 ± 34.384	0.093 ± 1.794	-.199	.961
C2-C3	Lat Flex	TPA	0	48.377 ± 27.984	7.964 ± 3.170	.470	.125
C3-C4	Lat Flex	TPA	0	139.875 ± 19.771	-2.813 ± 2.453	.050	.425
C4-C5	Lat Flex	TPA	0.932	134.330 ± 6.928	-3.119 ± 0.665	.778	.038
C5-C6	Lat Flex	TPA	0	154.347 ± 13.145	-6.273 ± 2.287	.521	.125
C6-C7	Lat Flex	TPA	1	123.624 ± 11.355	-3.499 ± 1.787	.321	.188
C7-T1	Lat Flex	TPA	0	74.045 ± 23.332	2.424 ± 5.215	-.186	.777
C2-C3	Lat Flex	UH	0	-2.188 ± 1.259	0.081 ± 0.143	-.128	.821
C3-C4	Lat Flex	UH	0	-1.832 ± 0.957	0.045 ± 0.119	-.167	.821
C4-C5	Lat Flex	UH	0	-1.931 ± 0.922	0.051 ± 0.120	-.158	.821
C5-C6	Lat Flex	UH	0	-1.456 ± 0.951	-0.039 ± 0.165	-.187	.821
C6-C7	Lat Flex	UH	0	-1.222 ± 1.121	-0.092 ± 0.220	-.159	.821
C7-T1	Lat Flex	UH	0	-1.288 ± 1.019	-0.057 ± 0.225	-.306	.821
C0-C1	Flex-Ext	SAFA	0.886	129.350 ± 5.072	-0.075 ± 0.119	-.112	.577
C0-C1	Flex-Ext	SAFH	0.911	-0.606 ± 0.123	0.005 ± 0.003	.309	.181
C1-C2	Flex-Ext	SAFH	0.231	-0.406 ± 0.119	-0.001 ± 0.006	.423	.128
C2-C3	Flex-Ext	SAFH	0	-0.561 ± 0.085	0.005 ± 0.005	-0.007	.479
C3-C4	Flex-Ext	SAFH	0.257	-0.696 ± 0.101	0.016 ± 0.006	.385	.098
C4-C5	Flex-Ext	SAFH	0	-0.681 ± 0.060	0.012 ± 0.003	.578	.032
C5-C6	Flex-Ext	SAFH	0.164	-0.588 ± 0.157	0.007 ± 0.008	-.030	.484
C6-C7	Flex-Ext	SAFH	0.697	-0.534 ± 0.154	0.003 ± 0.006	-.080	.625
C7-T1	Flex-Ext	SAFH	0	0.012 ± 0.187	-0.018 ± 0.008	.370	.174

Abbreviations: Ext, extension; Flex-Ext, flexion-extension; Lat Flex, lateral flexion; SAFA, superior articular facet angle; SAFH, superior articular facet height; SPA, spinous process angle; SPL, spinous process length; TPA, transverse process angle; TPL, transverse process length; UH, uncinat process height.

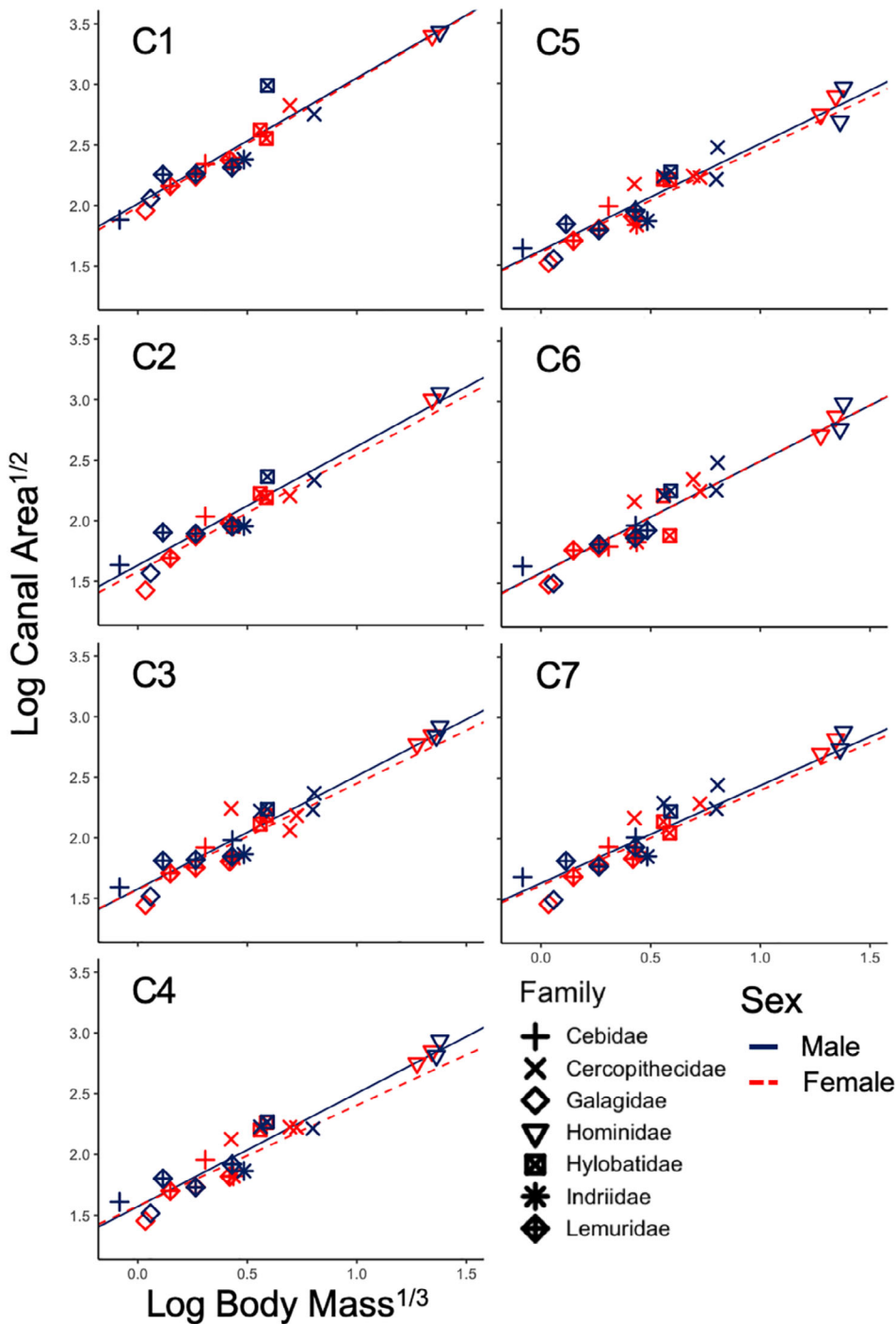


FIGURE 6 Phylogenetic generalized least-squares (PGLS) regressions between vertebral canal area within this sample and body mass collected from the literature (Smith & Jungers, 1997). All regressions are significant with high p -values, see Table 4

chimpanzees included in this study often used a combination of vertebral rotation and extension to achieve maximum dorsal inclination of the head. Knowledge of coupled motions, during locomotion and other habitual positional behaviors, would further our understanding of the influences of bony morphology on intervertebral ranges of motion.

The value of using 3D ROM has recently been demonstrated by Manafzadeh and Padian (2018). They investigated the degree to which ligaments restrain quail hip mobility in an effort to retrodict hip posture in fossil ornithodirans. They obtained an osteological measure of hip ROM by overlaying 3D scans of the hip and femur

and eliminating those overlays in which bones touched or the joint was dislocated. Ligamentous ROM was measured through manipulating dissected specimens and manipulating them in front of an XROMM system. They then mapped the ligamentous point cloud of possible osteological and ligamentous positions and found that ligaments restrict bony movement to 5.28% of the morphospace (Manafzadeh & Padian, 2018). This immense reduction in ROM underscores the function of ligaments: to provide joint stability. Our results, coupled with those of Manafzadeh and Padian (2018), strongly suggest that skeletal morphology rarely provides a bony stop for ROM.

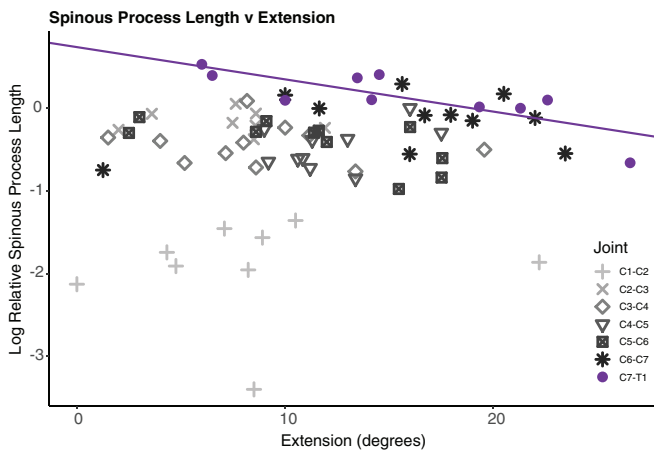


FIGURE 7 Phylogenetic generalized least-squares (PGLS) results of spinous process length (SPL) on maximum range of flexion per vertebral level. The significant result (C7-T1) is colored while nonsignificant correlations are in gray, see Table 5 for regression equations

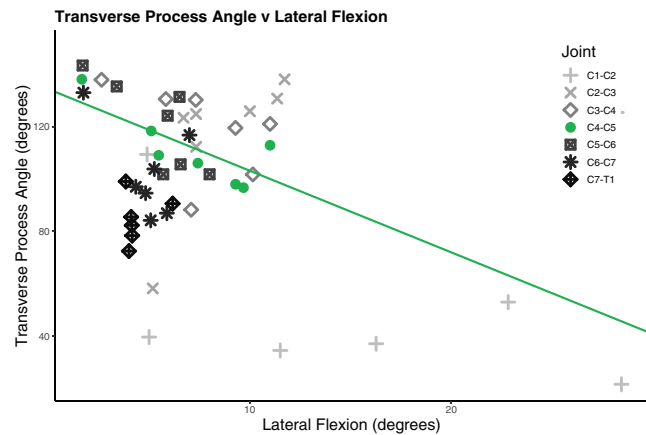


FIGURE 8 Phylogenetic generalized least-squares (PGLS) results of transverse process angle (TPA) on maximum range of lateral flexion per vertebral level. The significant correlation (C4-C5) is colored, and nonsignificant correlations are in gray see Table 5 for regression equations

5 | CONCLUSION

Overall, there is only a weak correlation between vertebral morphology and intervertebral ROM. Long spinous processes may inhibit neck extension but only at the cervicothoracic junction, long transverse processes may facilitate lateral flexion in the mid-cervical column, and articular facet height could facilitate flexion-extension. However, these associations are weak and indicate that bony morphology does not strongly predict vertebral ROM and should not be used to reconstruct ROM, especially in extinct species. Rather, it is likely that soft tissues—ligaments, vertebral discs, and musculature—are the primary determinants of joint motion. Future work should investigate the relative contribution of ligaments and intervertebral discs to providing intervertebral joint stability, especially in three-dimensions.

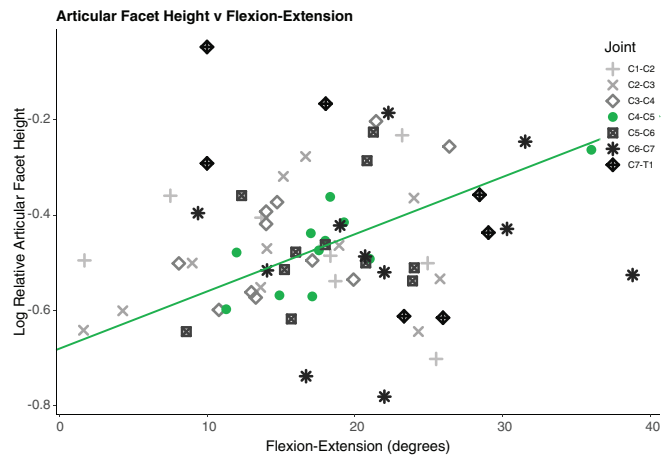


FIGURE 9 Phylogenetic generalized least-squares (PGLS) results of superior articular facet height (SAFH) on maximum range of flexion-extension per vertebral level. The significant regression (C4-C5) is colored and nonsignificant results are shades of gray see Table 5 for regression equations

ACKNOWLEDGMENTS

The authors would like to thank all those who helped with animal care and use including Dave Brewer, Erin Ehmke, Bobby Schopler, and Erin Shaw. The authors would also like to thank curators and staff at the following institutions for access to skeletal specimens: Eileen Westwig at the American Museum of Natural History, Arleyn Simon at Arizona State University, Eishi Hirasaki at Kyoto University, Jacques Cuisin at Muséum national d'Histoire naturelle, and Darrin Lunde at the National Museum of Natural History. This research was funded by American Association of Anatomists, Arizona State University's Graduate and Professional Student Association, the Japan Society for the Promotion of Science (SP15021), and the National Science Foundation (0935321, 1515271, and 1731142). The authors would also like to thank William Kimbel, David Raichlen, Gary Schwartz, and Carol Ward for their helpful discussion invaluable assistance in the thesis (Grider-Potter, 2019) from which this project originates. Finally, the authors appreciate the assistance of the two anonymous reviewers who improved the quality of this manuscript.

DATA AVAILABILITY STATEMENT

Range of motion data used in this study are available in Table 2. Skeletal morphometric data have been published in the dissertation from which this research originated (Grider-Potter, 2019).

ORCID

Neysa Grider-Potter  <https://orcid.org/0000-0002-9065-3739>

Thierra K. Nalley  <https://orcid.org/0000-0002-4296-2940>

Nathan E. Thompson  <https://orcid.org/0000-0002-9273-3636>

REFERENCES

- Aiello, L. C., & Dean, M. C. (2002). *An introduction to human evolutionary anatomy*. London: Elsevier Academic Press.
- Ankel, F. (1972). Vertebral morphology of fossil and extant primates. In *The functional and evolution biology of primates*. New York: Routledge (pp. 233–240).

- Arnold, C., Matthews, L. J., & Nunn, C. L. (2010). The 10kTrees website: A new online resource for primate phylogeny. *Evolutionary Anthropology*, 19, 114–118.
- Badoux, D. M. M. (1968). Some notes on the curvature of the vertebral column in vertebrates with species reference to mammals. *Acta Morphologica Neerlando-Scandinavica*, 7, 29–40.
- Benjamini, Y., & Hochberg, Y. (1995). Controlling the false discovery rate: A practical and powerful approach to multiple testing. *Biometrika*, 61, 289–300.
- Chow, D. H. K., Luk, K. D. K., Evans, J. H., & Leong, J. C. Y. (1996). Effects of short anterior lumbar Interbody fusion on biomechanics of Neighboring segments. *Spine (Phila Pa 1976)*, 21, 549–555.
- Eck, J. C., Humphreys, S. C., Lim, T. H., Jeong, S. T., Kim, J. G., Hodges, S. D., & An, H. S. (2002). Biomechanical study on the effect of cervical spine fusion on adjacent-level intradiscal pressure and segmental motion. *Spine (Phila Pa 1976)*, 27, 2431–2434.
- Gómez-Olivencia, A., Been, E., Arsuaga, J. L., Stock, J. T., Luis, J., & Stock, J. T. (2013). The Neandertal vertebral column 1: The cervical spine. *Journal of Human Evolution*, 64, 608–630.
- Gommery, D. (2000). Superior cervical vertebrae of a Miocene hominoid and a Plio-Pleistocene hominid from southern Africa. *Paleontologia Africana*, 36, 139–145.
- Graf, W., de Waele, C., & Vidal, P. P. (1995). Functional anatomy of the head-neck movement system of quadrupedal and bipedal mammals. *Journal of Anatomy*, 186, 55–74.
- Grider-Potter, N. (2019). Form and function of the primate cervical vertebral column (Doctoral Dissertation). Arizona State University, Tempe, AZ.
- Grider-Potter, N., & Hallgren, R. C. (2013). Atlantooccipital joint orientation and posture in catarrhines. *American Journal of Physical Anthropology*, 556, 137.
- Hamrick, M. W. (1996). Articular size and curvature as determinants of carpal joint mobility and stability in strepsirrhine primates. *Journal of Morphology*, 127, 113–127.
- Harmon, L., Weir, J., Brock, C., Glor, R., Challenger, W., Hunt, G., ... Eastman, J. (2008). GEIGER: Investigating evolutionary radiations. *Bioinformatics*, 24, 129–131.
- Heuer, F., Schmidt, H., Klezl, Z., Claes, L., & Wilke, H. J. (2007). Stepwise reduction of functional spinal structures increase range of motion and change lordosis angle. *Journal of Biomechanics*, 40, 271–280.
- Hilibrand, A. S., & Robbins, M. (2004). Adjacent segment degeneration and adjacent segment disease: The consequences of spinal fusion? *The Spine Journal*, 4, 190–194.
- Jonas, R., & Wilke, H.-J. (2018). *The cervical spine*. In: Galbusera, F. and Wilke H-J (Eds) *Biomechanics of the Spine*. London: Academic Press (pp. 11–34).
- Kapandji, I. A. (2008). The cervical spine. In *The physiology of joints: The vertebral column, pelvic girdle, and head*. London: Churchill Livingstone (pp. 186–274).
- Kumar, M., Baklanov, A., & Chopin, D. (2001). Correlation between sagittal plane changes and adjacent segment degeneration following lumbar spine fusion. *European Spine Journal*, 10, 314–319.
- MacLarnon, A. (1996). The evolution of the spinal cord in primates: Evidence from the foramen magnum and the vertebral canal. *Journal of Human Evolution*, 30, 121–138.
- MacLarnon, A. N. N., & Hewitt, G. (2004). Increased breathing control: Another factor in the evolution of human language. *Evolutionary Anthropology*, 197, 181–197.
- Manafzadeh, A. R., & Padian, K. (2018). ROM mapping of ligamentous constraints on avian hip mobility: Implications for extinct ornithodirans. *Proceedings of the Royal Society B: Biological Sciences*, 285, 20180727.
- Manfreda, E., Mitteroecker, P., Bookstein, F. L., & Schaefer, K. (2006). Functional morphology of the first cervical vertebra in humans and nonhuman primates. *Anatomical Record. Part B, New Anatomist*, 289, 184–194.
- Meyer, M. R., Woodward, C., Tims, A., & Bastir, M. (2018). Neck function in early hominins and suspensory primates: Insights from the uncinate process. *American Journal of Physical Anthropology*, 166, 1–25.
- Milne, N. (1991). Zygapophyseal joint orientation reflects the role of uncinate processes in the cervical spine. *Proceedings of the Australasian Society for Human Biology*, 4, 171–186.
- Nalley, T. K. (2013). Positional behaviors and the neck: A comparative analysis of the cervical vertebrae of living primates and fossil hominoids (Doctoral Dissertation). Arizona State University, Tempe, AZ.
- Nalley, T. K., & Grider-Potter, N. (2015). Functional morphology of the primate head and neck. *American Journal of Physical Anthropology*, 156, 531–542.
- Nalley, T. K., & Grider-Potter, N. (2017). Functional analyses of the primate upper cervical vertebral column. *Journal of Human Evolution*, 107, 19–35.
- Onan, O. A., Heggenes, M. H., & Hipp, J. A. (1998). A motion analysis of the cervical facet joint. *Spine (Phila Pa 1976)*, 23, 430–439.
- Orme, A. D., Freckleton, R., Thomas, G., Petzoldt, T., Isaac, N., Pearse, W., & Orme, M. D. (2013). CAPER: Comparative analyses of phylogenetics and evolution in R. *Methods in Ecology and Evolution*, 3, 45–151.
- Panjabi, M., Dvorak, J., Crisco, J. J., Oda, T., Wang, P., & Grob, D. (1991). Effects of alar ligament transection on upper cervical spine rotation. *Journal of Orthopaedic Research*, 9, 584–593.
- Panjabi, M., Dvorak, J., & Iii, J. C. (1991). Flexion, extension, and lateral bending of the upper cervical spine in response to alar ligament transections. *Journal of Spinal Disorders*, 4, 157–167.
- Paradis, E., Blomberg, S., Bolker, B., Brown, J., Claude, J., Cuong, H. S., de Vinne, D. (2018). Ape 5.0: An environment for modern phylogenetics and evolutionary analyses in R. *Bioinformatics*, 35, 526–528.
- Parks, H. (2012). Functional morphology of the atlas in primates and its implications for reconstructing posture in fossil taxa (Masters Thesis). Western Illinois University, Macomb, IL.
- Rohmann, A., Zander, T., Schmidt, H., Wilke, H. J., & Bergmann, G. (2006). Analysis of the influence of disc degeneration on the mechanical behaviour of a lumbar motion segment using the finite element method. *Journal of Biomechanics*, 39, 2484–2490.
- Schneider, C. A., Rasband, W. S., & Eliceiri, K. W. (2012). NIH image to ImageJ: 25 years of image analysis. *Nature Methods*, 9, 671–675.
- Schultz, A. H. (1942). Conditions for balancing the head in primates. *American Journal of Physical Anthropology*, 29, 483–497.
- Schultz, A. H. (1961). Vertebral column and thorax. *Primatologia*, 4, 1–66.
- Smith, R. J., & Jungers, W. L. (1997). Body mass in comparative primatology. *Journal of Human Evolution*, 32, 523–559.
- Strait, D. S., & Ross, C. F. (1999). Kinematic data on primate head and neck posture: Implications for the evolution of basicranial flexion and an evaluation of registration planes used in paleoanthropology. *American Journal of Physical Anthropology*, 108, 205–222.
- Toerien, M. J. (1961). The length and inclinations of the primate cervical spinous process. *Transactions of the Royal Society of South Africa*, 36, 95–105.
- White, A., & Panjabi, M. M. (1990). *Clinical biomechanics of the spine*. Philadelphia, PA: J.B. Lippincott Company.

How to cite this article: Grider-Potter N, Nalley TK, Thompson NE, Goto R, Nakano Y. Influences of passive intervertebral range of motion on cervical vertebral form. *Am J Phys Anthropol*. 2020;1–14. <https://doi.org/10.1002/ajpa.24044>